RESEARCH

Extreme drought triggers parallel shifts in wood anatomical and physiological traits in upper treeline of the Mediterranean Andes

Luiz Santini Jr.[1], Dylan Craven[2,3], Daigard Ricardo Ortega Rodriguez[4], Manolo Trindade Quintilhan[5], Stephanie Gibson-Carpintero[6], Cristina Aravena Torres[1], Fidel A. Roig[1,7], Ariel A. Muñoz[8] and Alejandro Venegas-Gonzalez[1,9*]

Abstract

Background Treeline ecotones of Mediterranean ecoregions have been affected by the increasing intensity and severity of droughts. Even though the effect of droughts on forest dynamics has been widely documented, knowledge is relatively scarce of how extreme climate episodes affect the hydraulic structure and, therefore, the physiology of woody plants. The Mediterranean Andes have experienced an uninterrupted period of drought since 2010, including an extremely dry year in 2019 with approximately 80% rainfall deficit. Here, we investigated shifts in wood anatomical and physiological traits of *Kageneckia angustifolia*, an endemic treeline species, in response to this drought period.

Methods We evaluated the xylem plasticity of three *K. angustifolia* populations across their natural distribution (31–35° SL) based on anatomical (vessel structure and distribution) and physiological (intrinsic water-use efficiency) variables in the tree rings. We focused on the period 2000–2020 that corresponds to before the megadrought (2000–2007), (ii) megadrought (2008–2018) and (iii) hyperdrought (2019–2020). The variables were annualized and analyzed by linear mixed-effects models.

Results Our results provide insights to the anatomical and physiological mechanisms underlying the resilience of treeline forests to persistent droughts in central Chile. We found that the extreme drought in 2019–2020 triggered shifts in vessel size and frequency that increased hydraulic safety. These significant shifts in vessel traits occurred in parallel with a decrease in pit aperture area and an increase in water-use efficiency, further increasing the resilience of *K. angustifolia* to extreme drought stress.

Conclusions Our results revealed coordinated shifts in vessel size and frequency and water-use efficiency in response to the megadrought, thereby reducing vulnerability to hydraulic failure. The apparent resilience of *K. angustifolia* to extreme droughts suggests that this adaptation to drought stress may increase its ability to tolerate novel climatic conditions of treeline environments of the Mediterranean Andes, although it is not clear whether these adaptations will be sufficient to persist in scenarios that predict intensification of climate stress. Finally, our results provide empirical evidence that integrating wood anatomical and physiological traits facilitates the understanding of resilience mechanisms that treeline forests develop in the face of increasing drought stress.

Keywords Dendro-anatomy, *Kageneckia angustifolia*, Xylem vulnerability, Drought, Climate change

*Correspondence:
Alejandro Venegas-Gonzalez
alejandro.venegas@uoh.cl
Full list of author information is available at the end of the article

Santini Jr. *et al. Ecological Processes*   (2024) 13:10

Page 2 of 12

Introduction

Treeline ecotones in upper mountain ecosystems are affected by increasing intensity and severity of droughts and global warming, especially in Mediterranean ecoregions (Garreaud et al. 2020; Cook et al. 2022; González-Reyes et al. 2023). Even though the effect of droughts on montane ecosystems has been widely documented (Granda et al. 2018; Colangelo et al. 2021; Matskovsky et al. 2021; Gazol et al. 2022), knowledge is relatively scarce of how extreme climate episodes affect the hydraulic structure and, therefore, the physiology of woody plants. Therefore, it is relevant to understand how extreme drought phenomena affect the level of resilience of forests in contexts of climate crisis.

Due to the rapid climate changes that Mediterranean ecosystems are experiencing and their future predictions of intensification (Seager et al. 2019), upper treelines constitute a model system to evaluate resilience capacities through modifications of xylem anatomical traits and physiological processes (Pepin et al. 2015; McDowell et al. 2022). Drought-driven declines in ring growth are directly influenced by changes in cellular structure of wood, whose xylem structure captures inter-annual growth patterns (Fonti et al. 2010). The xylem anatomical functional traits provide deeper information than just the analysis of the variation in ring widths (Beeckman 2016; Gennaretti et al. 2022). The size and frequency of the vessels (Garcia-Gonzalez et al. 2016), as well as the structure of their interconnections (Mrad et al. 2018) are indicators of the hydraulic conductivity and carbon allocation capacities, both at the level of interannual and interspecific variations (Cuny et al. 2015; Zwieniecki and Secchi 2015). In parallel with temporal changes in vessel structure and distribution, intrinsic water-use efficiency (iWUE) relates atmospheric carbon uptake through photosynthesis to water loss through transpiration, reflecting physiological responses to water stress over time (Lavergne et al. 2020; Cherubini et al. 2021). Therefore, by integrating anatomical traits of wood linked to safety and hydraulic efficiency with physiological traits of the xylem (Pellizzari et al. 2016), it facilitates the understanding of the resilience mechanisms that treeline forests develop in the face of extreme climatic events, which is the primary purpose of this work (Martínez-Vilalta et al. 2023).

In central Chile, treeline ecosystems are susceptible to droughts, with incidence in growth, reproduction and survival dynamics (Cavieres et al. 2021; Matskovsky et al. 2021; Tovar et al. 2022). This region, the only one in South America with Mediterranean forests, has been experiencing increasingly severe and persistent droughts. Since 2010, precipitation has consistently remained below historical averages (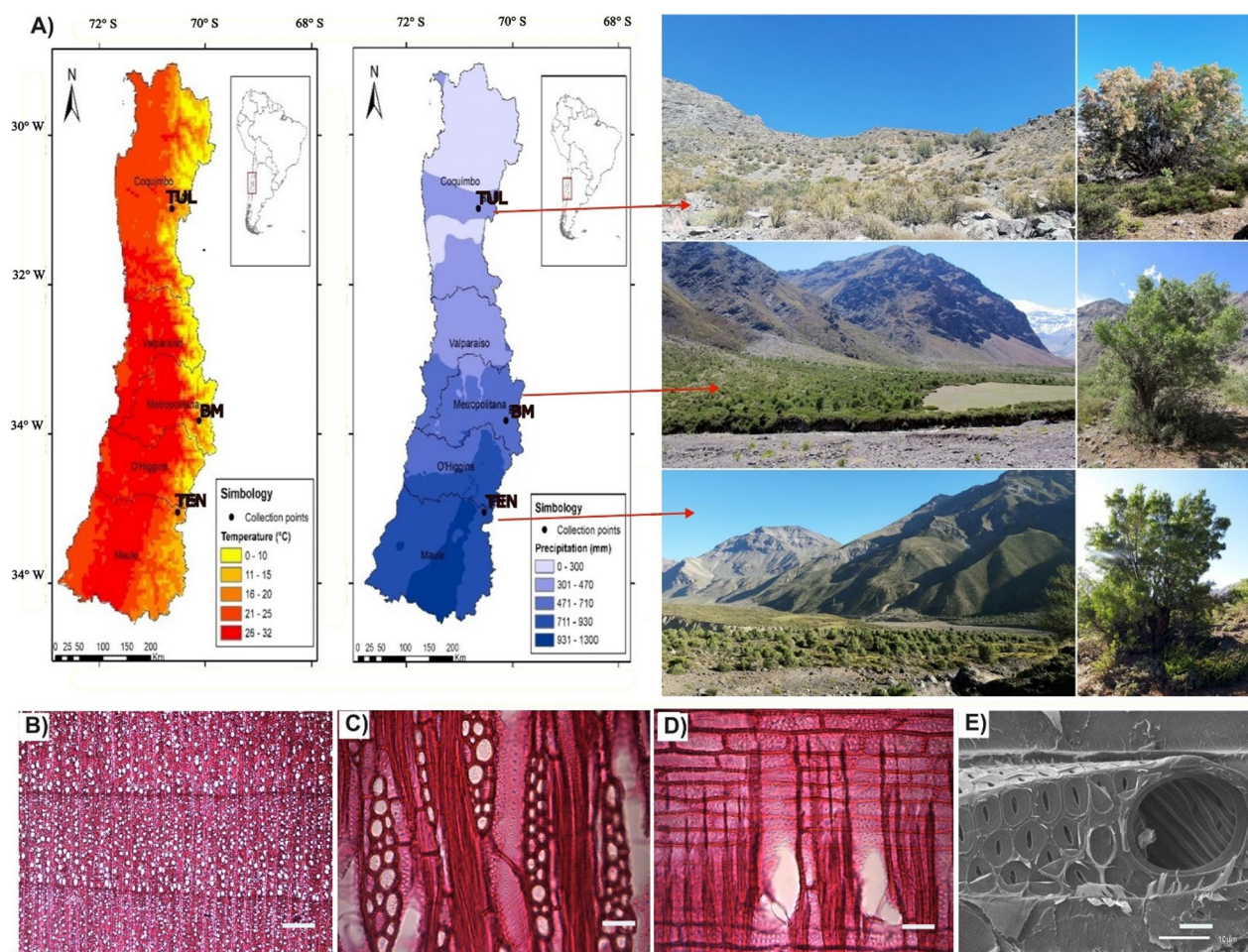Garreaud et al. 2020), including years of extreme drought, such as 2019, where the precipitation deficit was approximately 80% (Alvarez-Garreton et al. 2021). Forest ecosystems throughout the Mediterranean region of central Chile have been strongly affected by these persistent droughts, with significant declines in growth (Venegas-González et al. 2023), weakening of plant–pollinator interactions (Arroyo et al. 2020), and more extensive areas of forests with symptoms of 'browning' (Miranda et al. 2020). However, the anatomical and physiological mechanisms that underpin tree responses to persistent and increasingly severe droughts in central Chile and other Mediterranean regions are still poorly understood.

In this study, we examined shifts in wood anatomical and physiological traits of *Kageneckia angustifolia,* an endemic tree species distributed across the treeline in the Mediterranean Andes, in response to persistent droughts for period 2010–2020. Combining a wide range of anatomical and physiological traits of *K. angustifolia* wood, the following hypotheses were evaluated: the hydraulic system of stems is modified by the incidence of persistent droughts, by forming a greater number of vessels but with a smaller diameter (e.g.,García-Cervigón et al. 2018; Castagneri et al. 2020) and reducing the inter-vessel pit area (e.g., Lens et al. 2011); and water use efficiency (iWUE) increases as the water stress gradient intensifies (e.g., Lévesque et al. 2014; Peñuelas et al. 2011). To explore these hypotheses, we: (i) built tree-ring chronologies to exactly determine the calendar dating of the ring widths and analyze the tree growth rate, (ii) built vessel chronologies for the period 2000–2020, and (iii) evaluated temporal variation in vessel features and iWUE patterns in response to droughts of increasing severity.

Materials and methods

Study site and climate

We selected three sites of *K. angustifolia* across the Mediterranean Andes of central Chile (31–35° SL), to cover its entire natural distribution. This species, despite having a wide distribution ~ 400 km latitude, is limited to small forest patches at the treelines of the Mediterranean Andes between 1500 and 2300 m a.s.l. (Piper et al. 2006). In each site, we took samples of a *K. angustifolia* population, which has the following features: (i) northern population, located in Tulahuen (TUL, − 30.99°S, − 70.64°W, 1900 m a.s.l.), with an average annual precipitation of 100 mm yr^{-1} and temperature of 16.5 °C; (ii) central population, located in Baños Morales (BM, − 33.8° SL, − 70.1° WL, 1800 m a.s.l.), with average rainfall of 350 mm yr^{-1} and temperature of 14.6 °C; (iii) southern population, located in Teno (TEN, − 35.1° SL, − 70.5° WL, 1,600 m a.s.l.), has an average annual rainfall of 550 mm yr^{-1} and a temperature of 12.8 °C (Fig. 1A).

Santini Jr. *et al. Ecological Processes*   (2024) 13:10

Page 3 of 12

Fig. 1 **A** Map of three study sites located along gradients of temperature and precipitation in central Chile. Wood sections of *K. angustifolia*, **B** transversal (10x, bar = 500 μm), **C** tangential (40x, bar = 100 μm μm), and **D** radial (40x, bar = 100 μm). **E** Vessel element (2,200x, bar = 100 μm) showing the simple perforation plate and alternate inter-vessel pits

The wood anatomy of *K. angustifolia* populations demonstrates the high dendrochronological potential of the species, with semi-porous rings and increasing fiber wall thickness in latewood (Fig. 1B).

Sampling and processing of the ring-width chronologies
We sampled cores from the main stem and lateral branch discs closest to the base from 15 to 32 individuals of *Kageneckia angustifolia* at each study site (Table 1). The choice of collecting cores or branches of each tree was the following criteria: (i) when the main base was larger than the lateral branches, collecting with the increment borer was preferred, and (ii) when lateral branches were of a similar size to the main stem, we collected disks. In addition, we avoided selecting trees with damage, presence of pathogens, or reaction wood. Collections were made between February 2021 and April 2022. Wood

samples were processed according to standard procedures in dendrochronology (Stokes and Smiley 1968). Due to the similarity of tree heights within and between the study sites (Table 1), it was not necessary to vary the sampling point, as recommended by Carrer et al. (2015). Tree ring width measurements (RW) were performed using a Velmex measuring system with a resolution of 0.001 mm. The quality of the cross-dating was checked with COFECHA software (Grissino-Mayer 2001; Holmes et al. 1986). After building the ring width chronologies, we focused on the last two decades (2000–2020) to evaluate the effects of the intense drought that occurred in this period on wood anatomy and physiology.

Drought periods
We divided each sample into three periods, which differ in drought intensity as identified by Garreaud et al.

Santini Jr. *et al. Ecological Processes*   (2024) 13:10

Page 4 of 12

Table 1 Descriptive statistics for ring width chronologies and wood vessel traits across three populations of *K. angustifolia* (ring width and vessels features) in the Mediterranean Andes of central Chile

Variables	Sites		
	North	Central	South
Tree size			
DBH ± SD (cm)	13.98 ± 4.56	16.97 ± 5.45	14.11 ± 3.80
Height ± SD (m)	3.75 ± 0.85	4.00 ± 0.55	3.77 ± 0.98
Ring width chronology			
Total trees sampled	15	30	32
Total trees in chronology (radii)	15 (24)	26 (43)	26 (49)
Mean ring width ± SD (mm)	1.61 ± 1.01	2.06 ± 1.06	1.40 ± 0.76
Chronology span	1948–2020	1979–2020	1948–2020
Mean age (max–min)	50 (29–73)	28 (24–37)	56 (18–74)
Mean sensitivity	0.564	0.391	0.408
Series intercorrelation	0.568	0.530	0.556
RBar	0.340	0.280	0.305
Expressed population signal	0.941	0.880	0.942
Vessel traits			
Total trees studied	15	15	15
Mean vessel area ± SD (μm^2)	2650 ± 789a	3144 ± 1007b	3038 ± 978b
Mean vessel frequency ± SD (ind mm^{-2})	22.212 ± 6.750a	22.996 ± 7.650a	25.358 ± 8.468b
Mean hydraulic diameter (μm)	61.062 ± 9.264a	67.305 ± 11.270b	66.063 ± 11.274b
Mean K_p (kg m MPa^{-1} s^{-1})	2.814 ± 2.399a	3.817 ± 2.506b	5.738 ± 3.503c
Total vessel measured	18,755	19,644	18,238
Vulnerability index	$1.4E^{-5} \pm 1.0E^{-6}$a	$9.3E^{-6} \pm 1.2E^{-6}$b	$0.9E^{-5} \pm 2.0E^{-6}$b
Chronology span	2000–2020	2000–2020	2000–2020
Mean ring width ± SD (mm)	1.96 ± 1.04b	1.92 ± 1.00b	1.29 ± 0.80a

*Different letters indicate statistically significant differences between study sites, based on Kruskal–Wallis tests ($p < 0.05$)
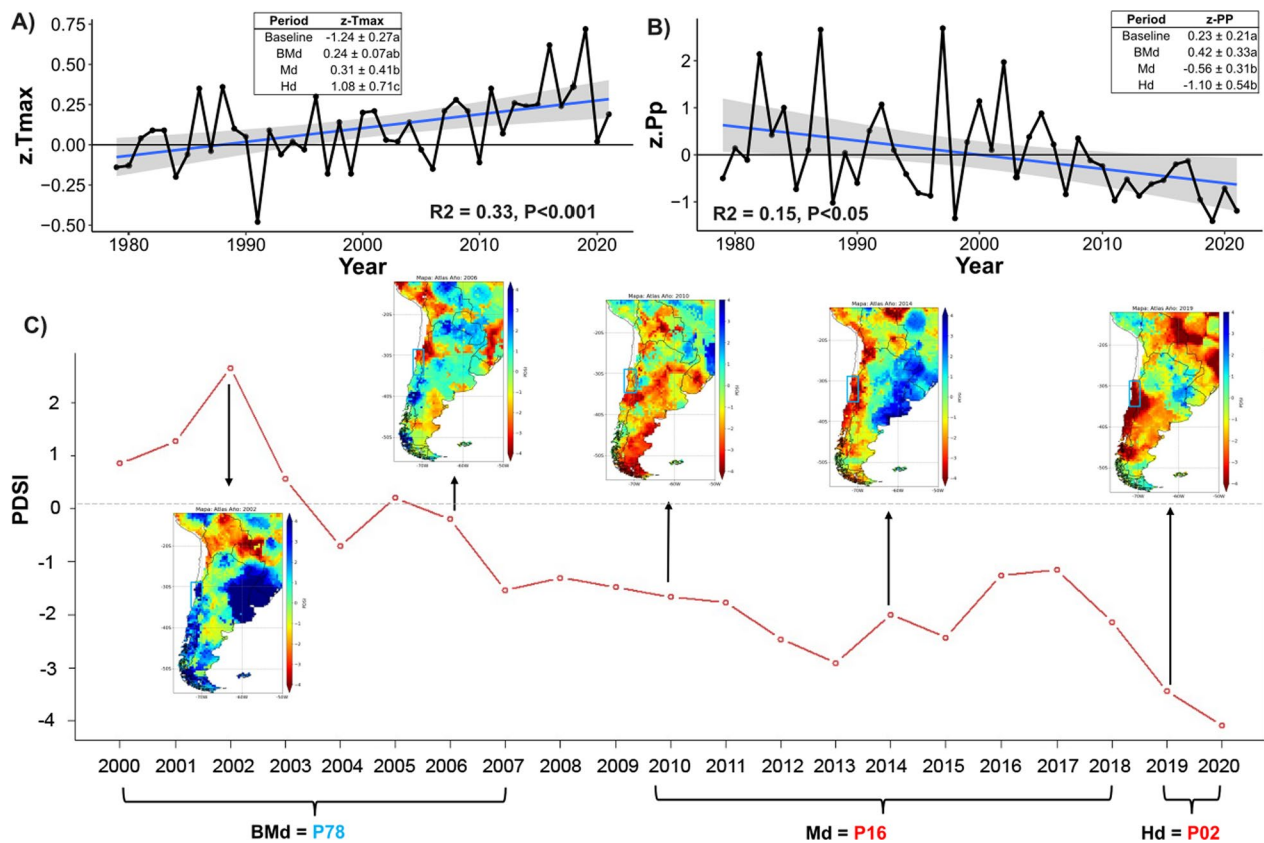
(2020) and Alvarez-Garreton et al. (2021): (i) reference period, before the megadrought (BMd: 2000–2007); (ii) the megadrought period (Md: 2010–2018), and (iii) the hyperdrought period (Hd: 2019–2020) (Fig. 2). We restricted the reference period (BMd) to 2000–2007, because Cook et al. (2022) showed a significant decline in soil moisture starting in 2008.

We further validated the selection of these periods by evaluating summer mean maximum temperature (Tmax), winter–spring total precipitation (Pp), and the Palmer Drought Severity Index (PDSI) (Additional file 1: Fig. S1). To evaluate temporal variation in Tmax and Pp, we used standardized data from four meteorological stations close to the three study sites, considering the period between 1979 and 2020. We fitted a generalized linear model (GLM) to evaluate the effect of the drought period on Tmax and Pp using the R function 'glm' (Bates et al. 2015). Comparisons among means for significant effects were made using Fisher's LSD tests ($p < 0.05$). We found statistically significant trends for both variables (Fig. 2). PDSI was analyzed using data from the South American Drought Atlas SADA (Morales et al. 2020). Based

on percentiles (Px) of PDSI for the period 1901–2020 for the study region (30.0–35.0° SL, 70.5–71.0° WL), we considered the baseline period of 2000–2007, because its drought severity was markedly lower than the two subsequent periods (Fig. 2C).

Wood anatomical traits
After building ring-width chronologies, we selected a subset of 45 samples (15 per site) to evaluate wood anatomical traits (in the case of northern site we included all trees sampled). We choose trees without defects or visible damage and without cross-dating problems. Wood samples from each individual were softened in a water/glycerin solution (4:1) and sectioned along the cross-sectional surface using a sliding microtome (Quintilhan et al. 2021). Sections were cleared with sodium hypochlorite (20%), dehydrated in an alcohol series (30–50%) and then stained with safranin (1%) (Santini Jr et al. 2019). We photographed samples with a digital camera coupled to an optical microscope (Digital Microscope Motic, software 2.0) and a magnification of 25x. We analyzed wood anatomical traits following the International Association of Wood Anatomists (IAWA)

Santini Jr. *et al. Ecological Processes*   (2024) 13:10

Page 5 of 12

Fig. 2 Climatic variability from 1979 to 2020 in central Chile: **A** z values of maximum temperature during the austral summer (December to February); **B** z values of precipitation in winter–spring (May–November). In both climatic series, mean values (± SE) across the drought periods are showed. **C** Annual Palmer Drought Severity Index for the study region (30–35°S, 70.5–71.0°W) for the period 2000–2020, with the three drought periods highlighted (*BMd* before megadrought, *Md* megadrought, *Hd* hyperdrought). We compared the three periods using percentiles (Px) from the period 1901–2020. In addition, we show the spatial variation of the PDSI in exceptional years using data from the South American Drought Atlas SADA (Morales et al. 2020)

standards. Measurements were performed by the ImageJ program (version 1.53a for Windows). We focused on earlywood vessels, because they provide better information on intra-annual variations of hydraulic traits (Fonti et al. 2010). Vessels larger than 40 μm diameter were measured in an area of 1.35 mm^2. Vessel frequency per mm^2 (VF) and mean vessel diameter (VD), were measured for each ring. The vulnerability index as the risk of hydraulic failure due to vessel characteristics (VI) (Carlquist 1977) was calculated with the following equation:

$$VI = \frac{VD}{VF} \tag{1}$$

Potential hydraulic conductivity (K_p), i.e., potential stem conductivity/ratio of stem conductivity, c.f. Hagen–Poiseuille law (Sterck et al. 2008), was also calculated with the following equation:

$$K_p = \pi \rho w / 128 \eta \times VF \times DH^4 \tag{2}$$

where K_p is the potential specific stem conductivity (kg m MPa^{-1} s^{-1}), η is the viscosity of water at 20 °C (1.002×10^{-3} Pa s at 20 °C), ρw is the density of water at 20 °C (998.2 kg m^{-3} at 20 °C), VF is the vessel frequency and D$_h$ is the hydraulically weighted vessel diameter (μm). DH was calculated with the following equation:

$$D_h = \frac{\sum_{n=1}^{N} d^5{}_n}{\sum_{n=1}^{N} d^4{}_n} \tag{3}$$

where d_n is the diameter of each vessel (Sperry et al. 1994). According to the Hagen–Poiseuille equation, D_h is linked to trade-off of hydraulic safety efficiency, which is negatively correlated with cavitation tension and, under current dry and hot environmental conditions, has high plasticity (Hacke and Sperry 2001).

Inter-vessel pits

We selected a subset of one wood core for each study site to evaluate variations in the inter-vessel pit size. We

Santini Jr. *et al. Ecological Processes*   (2024) 13:10

Page 6 of 12

selected samples with visibly marked rings and with a high correlation with the master series. Each core was cut into two small blocks that included the BMd and Hd period. We focused the measurements on radial and tangential surfaces (Fig. 1B, C). Samples were dried and fixed on aluminum stubs using carbon adhesive tape. Later, samples were sputter-coated with a 20-nm-thick gold blade using a sputter coater Denton Desk V (Denton Vacuum, USA) and analyzed with scanning electron microscopy (SEM, JSM 6610-LV, JEOL, Tokyo, Japan). In total, we measured 60 randomly selected pits (Fig. 1E), which correspond to 20 for each study site and 10 inter-vessel pits per period and per study site. The diameter of the pits and their elliptical apertures were measured using a magnification of 2000–20,000. We divided diameters by two to obtain the radius, which we then used to calculate the pit area and its aperture area using the ellipse formula ($\pi \times L_i \times W_i/4$). Finally, we worked on the variables pit total area and pit aperture area (Additional file 1: Fig. S1).

Wood intrinsic water-use efficiency (iWUE)

We selected a subset of 15 cores (5 individuals per study site) to analyze the $\delta^{13}C$ isotope composition for the period 2000–2020. We cut each core into three wood sections, each corresponding to the drought period considered in this study, e.g., BMd, Md, and Hd. To eliminate possible errors in the chemical process due to handling of the samples, we removed the upper surface of the wood using a sledge microtome (Gärtner and Nievergelt 2010). Samples were pooled by period and analyzed with an elemental analyzer–isotope ratio mass spectrometer (Flasha EA 112 coupled via Conflo IV to a Delta Plus XP mass spectrometer, Thermo Electron, Bremen, Germany). We used whole wood instead of cellulose, because previous studies on hardwood species showed that material from the sapwood is as useful as cellulose for studying environmental effects at a short-term scale (Weigt et al. 2015). Following international standards, we used Vienna Pee Dee Belemmnite. The carbon isotope ratio was calculated as

$$\delta^{13}C(\text{‰}) = \left[\left({}^{13}C/{}^{12}C_{\text{sample}} \right) / \left({}^{13}C/{}^{12}C_{\text{standard}} \right) - 1 \right] \times 1000.$$

We then calculated the wood intrinsic water-use efficiency (iWUE, µmol CO_2 mol^{-1} H_2O), carbon isotope discrimination ($\Delta^{13}C$, ‰) and intercellular CO_2 concentration (C_i, ppm), using the 'simple' formulation (Lavergne et al. 2022). We used 25.5‰ as the apparent fractionation for wood tissue (Cernusak and Ubierna 2022). All estimates were calculated using the R package 'isocalcR' (Mathias and Hudiburg 2022) for each period and individual, accounting for elevation, mean annual

temperature, and ambient CO_2 concentration. Mean annual temperature for each period was obtained from ERA5 re-analysis (Hersbach et al. 2020) for each study site.
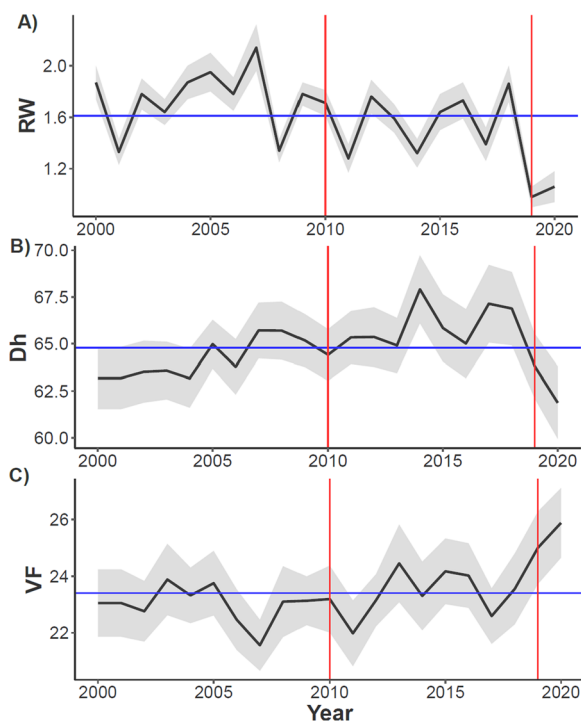
Statistical analysis

To examine variation in wood anatomical and physiological characteristics, we fitted linear mixed-effects models with drought period (BMd, Md and Hd), DBH (as a proxy for tree size), and the two-way interactions between them as fixed effects, and individual nested within sites as the random effect using the R-package 'lme4' (Bates et al. 2015) in software R (R Core Team 2020). We used the annualized variables to avoid problems with unbalanced data by period (Venegas-González et al. 2020), which was obtained by dividing the data by 8, 9 and 3 years for BMd, Md and Hd, respectively. To meet normality assumptions, ring width, K_p, and vulnerability index were log-transformed prior to analysis; we also log-transformed DBH to linearize its relationships with response variables. We assessed model assumptions using the 'check_model' function in the R package "performance" (Lüdecke et al. 2021), which provides visual evaluations of the normality of model residuals and random effects. Because the full model for wood iWUE and C_i was rank deficient, we removed the interaction with study site and period. Comparison among means for significant effects were evaluated using Fisher's LSD tests ($P < 0.05$).

Results

Tree-ring and vessel trait chronologies

The wood anatomy of *K. angustifolia* populations demonstrates the high dendrochronological potential of the species, with semi-porous rings and increasing fiber wall thickness in latewood (Additional file 1: Fig. S2). From the 77 trees sampled, 67 were successfully cross-dated (87%, $r = \sim 0.55$ and RBar $= \sim 0.31$) and were used to build the ring width chronologies for each population (Table 1). The northern and southern populations are comprised of adult trees with an average age of 53 years with a maximum age of 74 years, while the central population is younger (average age of 22 years). Annual growth, i.e., average tree-ring width, is similar across all populations, with mean values between 1.40 and 2.06 mm yr^{-1}.

We built chronologies of wood anatomical traits covering three periods of increasing drought severity across the range of *Kageneckia angustifolia* in central Chile (2000–2020, Fig. 3). In total, we analyzed 56,637 vessels of *K. angustifolia* trees for the period 2000–2020 (Table 1). We found smaller vessels, in terms of mean vessel area and hydraulic diameter, in the center and southern populations. On the other hand, the central and northern sites have the highest annual rates of radial growth, but

Fig. 3 Annual variation of **A** tree ring width (RW, mm yr^{-1}), **B** hydraulic diameter (D_h, μm) and **C** vessel frequency (VF, ind mm^{-2}) for the period 2000–2020. The black line is the mean and the shaded area is the standard error. Red vertical lines represent the start of the megadrought in 2010 and the extreme drought in 2019

lower vessel frequency, in contrast to what we observed in the southern population. The highest value of potential hydraulic conductivity (K_p) was found in the southern population, which was 104% and 50% higher than that of the northern and central populations, respectively. Consequently, we found the highest values of the vulnerability index in the northern population (Table 1).

Tree responses to drought intensity

We found that wood anatomical and physiological traits varied significantly in response to drought severity (Additional file 1: Table S1). In general, most of the total variation of each wood trait was explained by random effects, i.e., variation within study sites and individuals (conditional R^2: 0.58–0.88; marginal R^2: 0.04–0.39). All wood traits exhibited a statistically significant response to drought intensity. Furthermore, we found that hydraulic diameter (D_h), potential hydraulic conductivity (K_p), and ring width (RW) increased with increasing tree size (DBH) (Additional file 1: Fig. S3). In addition, the interaction between drought period and DBH was statistically significant for vessel frequency (VF) and the vulnerability index (VI) (Additional file 1: Fig. S4).

With increasing drought severity, radial growth (RW) and the vulnerability index (VI) declined significantly during the Hd period (Fig. 4A–E). In contrast, vessel frequency (VF) increased in response to drought intensity (Fig. 4B). Hydraulic diameter (D_h) and K_p increased during the megadrought period (Md), but decreased during the hyperdrought period (Hd), reaching values similar to those before the start of the megadrought period (BMd) (Fig. 4C, E). On other hand, iWUE increased with drought severity and was highest in the Hd period (Fig. 4F). We found that carbon isotope discrimination ($\Delta^{13}C$) also declined significantly on both drought periods, while C_i increased during the Hd period, but not significantly (Additional file 1: Table S1, Fig. S5).
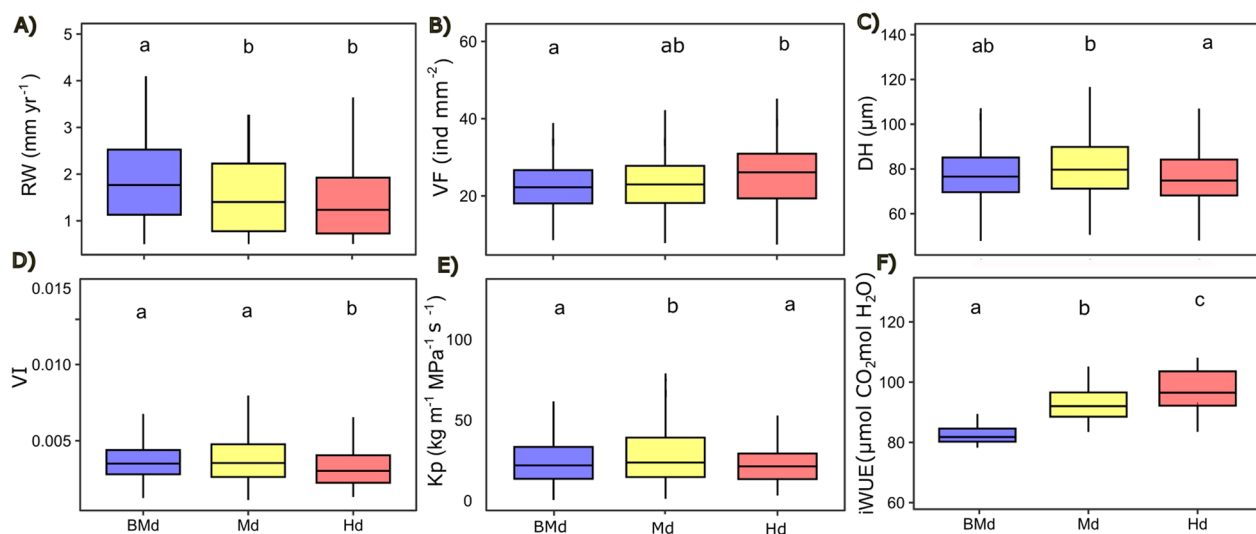
We only found significant differences between drought periods for inter-vessel pit aperture area, but not inter-vessel pit total area (Fig. 5, Additional file 1: Fig. S6). These differences are attributed to the reduction of the pits with respect to their length (19%), width (20.2%), and area (37.1%) during the Hd period.

Discussion

In this study, we explored the anatomical and physiological mechanisms that underpin the response of a treeline forest species of *K. angustifolia* to increasing drought intensity. Our results revealed coordinated shifts in vessel size and frequency and water-use efficiency to enhance the hydraulic safety. The apparent resilience of *K. angustifolia* to extreme droughts suggests that this adaptation to drought stress may increase its ability to tolerate novel climatic conditions at the treeline environments of the Mediterranean Andes.

Vessel traits in response to drought intensity

Consistent with previous studies (Barichivich et al. 2009), we found that the ring width decreased in response to the historic drought of 2019 (Fig. 4). This is likely due to the fact that during the formation of tree rings favorable climatic conditions allow for the formation of larger diameter vessels, which improves water transport capacity and leads to an increase in tree growth (Garcia-Gonzalez et al. 2016; Nola et al. 2020; Gennaretti et al. 2022). Our analysis identified evidence of shifts in vessel traits in response to drought severity that are consistent with greater hydraulic safety, underlying the decrease in ring width. Under harsh climate conditions, e.g., low precipitation and high temperatures, vessel frequency is expected to increase and vessel diameter to decrease, thereby increasing hydraulic safety as these changes reduce the risk of cavitation (Sperry et al. 2006; Choat et al. 2012; Gea-Izquierdo et al. 2012; Gleason et al. 2016). Particularly after the extreme drought in 2019–2020, we observed an increase in vessel frequency and
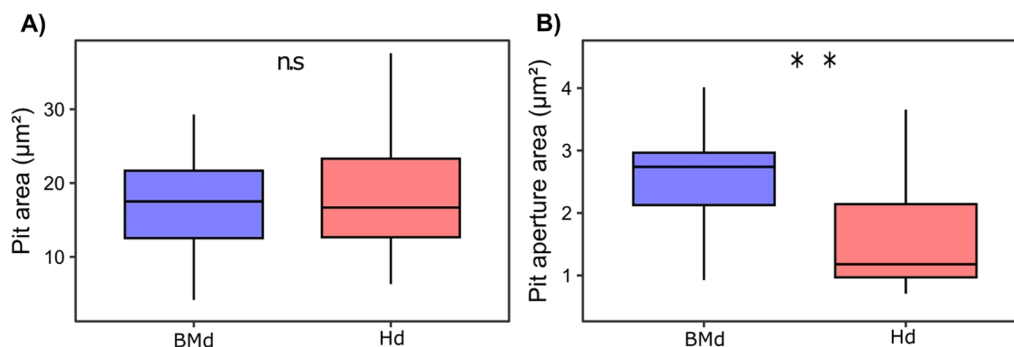
Fig. 4 Estimated values of wood anatomical and physiological traits of *K. angustifolia* populations across drought periods (before megadrought—BMd: 2000–2007, megadrought period—Md: 2010–2018, hyperdrought period—Hd: 2019–2020. **A** Ring width (RW, mm yr^{-1}); **B** vessel frequency (VF, ind mm^{-2}); **C** hydraulic diameter (DH, µm); **D** vulnerability index of the xylem to embolism (VI); **E** potential hydraulic conductivity (K_p, kg m MPa^{-1} s^{-1}); **F** wood intrinsic water-use efficiency (iWUE; µmol CO_2 mol^{-1} H_2O). Differences between periods for each site were evaluated using Fisher's LSD test ($p < 0.05$)

a decrease in hydraulic diameter, both aspects linked to increasing hydraulic safety (Fig. 3). These changes in vessel traits likely reduce the vulnerability of *K. angustifolia* to cavitation as evidenced by the decrease in the vulnerability index, which captures vessel diameter to frequency ratio (Fig. 3D). However, we also found that during the hyperdrough period (Hd) there was a decrease in potential hydraulic conductivity, indicating a reduction in lumen area, which likely decreases stem (Bryukhanova and Fonti 2013). Previous studies focused on conifers have shown lower theoretical hydraulic conductivity, suggesting a long-lasting process of hydraulic deterioration in their water transport system, that could be linked to crown dieback and a decline in tree vigor (Pellizzari

et al. 2016; Puchi et al. 2021). Consequently, it is necessary to continue monitoring these populations. Furthermore, we found that the decrease in D_h and K_p observed between the Md and Hd periods is not due to ontogeny, and rather, could indicate a pre-adaptive response of the species to this historical climatic event.

The observed shift towards a greater efficiency of the hydraulic safety in response to drought severity could be due to the fact that species' range is restricted to high elevations, consistent with the 'pre-adaptation hypothesis' (Peñuelas et al. 2001; De Kort et al. 2020), where tree growth rates are typically lower than species that occur at lower elevations (Körner and Hoch 2023). Even under normal environmental conditions, tree species of

Fig. 5 Boxplots of inter-vessel pit area and inter-vessel pit aperture area of studied *K. angustifolia* trees between the periods: **A** before the megadrought (BMd: 2000–2007), and **B** the hyperdrought period (Hd: 2019–2020). **Indicate significant differences between period with $p < 0.01$

Santini Jr. *et al. Ecological Processes*   (2024) 13:10

Page 9 of 12

Mediterranean mountain forests of central Chile have exhibited slow radial growth rates, which are lower than 1.5 mm yr^{-1} (Venegas-González et al. 2018; Matskovsky et al. 2021). Moreover, *K. angustifolia*, as a semi-ring-porous species, produces earlywood with wider vessels (Fig. 1B), which is associated with greater xylem plasticity, which in turn facilitates greater hydraulic efficiency (García-González et al. 2016; Rodríguez-Ramírez et al. 2022).

Further supporting the shift towards greater hydraulic safety, our results indicate a decrease in pit aperture area with increasing drought intensity. The trade-off between safe and efficient xylem transport is related to protection against blockage from cavitation and embolism, and low flow resistance for the vascular tissue (von Arx et al. 2016), which inferred directly changes in pit membranes (Wheeler et al. 2005; Mrad et al. 2018). Smaller elliptical pit apertures have been found to be positively correlated with enhanced resistance to cavitation (Schmitz et al. 2007; Lens et al. 2011; Zhang et al. 2017). Wheeler et al. (2005) found an inverse relationship between the pit surface area per vessel and water potential, inducing tradeoffs between xylem safety and hydraulic efficiency for eleven tree species of the Rosaceae family, the same family as that of *K. angustifolia* (Hacke et al. 2006; Choat et al. 2008; Pittermann et al. 2010; Lens et al. 2011). Together with the plastic responses of vessel traits to increased drought intensity, the decrease in pit aperture area supports the idea that *K. angustifolia* is resilient to water stress, which supports the pre-adaptation hypothesis, i.e., that species or populations that evolve in stressful environments have a high capacity to adapt to climate change (Li et al. 2018; Xu et al. 2020).

iWUE in response to drought intensity

We found that *K. angustifolia* increased wood iWUE in response to increasing drought intensity. This response supports the idea that *K. angustifolia* exhibits a drought avoidance strategy (Martínez-Ferri et al. 2000), by closing its stomata to reduce transpiration (Saurer and Voelker 2022). In line with our results, declines in tree growth and increases in iWUE in other high-elevation Mediterranean forests have been observed in recent decades in response to global change (Andreu-Hayles et al. 2011; Peñuelas et al. 2011; Granda et al. 2014; Wu et al. 2015). In contrast, forests that have experienced drought-induced mortality have shown an increase in $\Delta^{13}C$ and a decrease in iWUE, suggesting higher stomatal conductance rates (Linares and Camarero 2012; Hentschel et al. 2014; López et al. 2021). Therefore, our results suggest that *K. angustifolia* has largely avoided drought induced mortality via a reduction in stomatal conductance and shift in vessel traits towards greater hydraulic safety. As

the drought in our study region has continued since 2020, it remains unclear the extent to which *K. angustifolia* will be able to continue tolerating water stress.

Conclusions

Our study provides insights to the anatomical and physiological mechanisms underlying the resilience of tree-line forests to persistent droughts in central Chile. We found that the extreme drought in 2019–2020 triggered shifts in vessel size and frequency and frequency that increased hydraulic safety, thereby reducing vulnerability to hydraulic failure. These shifts in vessel traits occurred in parallel with a decrease in pit aperture area and an increase in water-use efficiency, further increasing the resilience of *K. angustifolia* to drought stress. Therefore, our results suggest a high capacity of *K. angustifolia* to tolerate droughts, even though it is not clear whether these adaptations will be sufficient to scenarios of greater intensification of climate stress in the future. Given the extent of the impacts of the megadrought on tree growth and productivity of Mediterranean forests in central Chile, it is crucial to extend the analysis of drought responses to other tree species in these ecosystems, which will allow us to test if other high-elevation species also exhibit a greater capacity to tolerate droughts. Furthermore, examining non-structural carbohydrate (NSC) dynamics during the megadrought may further elucidate the capacity of tree species in these ecosystems to endure persistent droughts.

Abbreviations

BMd	Before megadrougth
Md	Megadrougth
Hd	Hyperdrought
VF	Frequency of vessels
Dh	Hydraulic diameter
RW	Tree-ring width
VI	Vulnerability index
Kp	Potential hydraulic conductivity
iWUE	Intrinsic water-use efficiency

Supplementary Information

Additional file 1: Fig. S1. Measurements of length and width of inter-vessel pits and their apertures of *Kageneckia angustifolia*, using different zoom x. (A) 3,000x, (B) 9,000x, (C) 11,000x, and (D) 19,000x. The pit total area and pit aperture area were calculated as π×L_t×W_t/4. **Fig. S2.** Mean index residual chronologies (black series), numbers of series (light gray series) and EPS values (dashed line shows the arbitrary 0.85 EPS threshold) of *Kageneckia angustifolia* for (A) North, (B) Central, and (C) South populations. All sites had high mean sensitivity (> 0.39) and expressed population signal values (> 0.85) (Table 1). **Fig. S3.** Shifts in wood anatomical and physiological traits of *K. angustifolia* populations with tree size. Solid lines indicate statistically significant fits ($p < 0.05$). Lines and 95% confidence intervals were fitted using linear mixed-effects models. (A) Ring width (mm yr^{-1}); (B) vessel frequency (VF, ind mm^{-2}); (C) hydraulic diameter

Santini Jr. *et al. Ecological Processes*   (2024) 13:10

Page 10 of 12

(DH, μm); (D) vulnerability index of the xylem to embolism (VI); (E) potential hydraulic conductivity (K_p, kg m MPa^{-1} s^{-1}); (F) wood intrinsic water-use efficiency (iWUE; μmol CO_2 mol^{-1} H_2O). Differences between periods for each site were evaluated using Fisher's LSD test ($p < 0.05$). **Fig. S4.** Estimated values of wood anatomical and physiological traits of *K. angustifolia* populations across study sites and among periods. Lines and 95% confidence intervals were fitted using linear mixed-effects models. (A) Ring width (mm yr^{-1}); (B) vessel frequency (VF, ind mm^{-2}); (C) hydraulic diameter (DH, μm); (D) vulnerability index of the xylem to embolism (VI); (E) potential hydraulic conductivity (K_p, kg m MPa^{-1} s^{-1}); (F) wood intrinsic water-use efficiency (iWUE; μmol CO_2 mol^{-1} H_2O). Differences between periods for each site were evaluated using Fisher's LSD test ($p < 0.05$). **Fig. S5.** Boxplot of (A) carbon isotope discrimination $\Delta^{13}C$ (‰), and (B) C_i (ppm) of *Kageneckia angustifolia* trees. Differences between periods for each site were evaluated according to Fisher's LSD test ($p < 0.05$). **Fig. S6.** Boxplot of length and width of inter-vessel pits and their apertures of studied *Kageneckia angustifolia* trees. (A) Pit length, (B) pit width, (C) pit aperture length, (D) pit aperture width. * Indicate significant differences between period with $p < 0.05$. **Table S1**. Parameters of LMMs evaluating the effect of drought period, tree size (DBH), and their interaction, on wood anatomical and physiological traits of *K. angustifolia*. Parameters are shown for *F* value (statistic) and *P* value, marginal *R*-squared (R_m^2) and conditional R-squared (R_c^2). Significant *P* values are shown in * (< 0.05). Vessel traits are ring width (RW), vessel frequency (VF), hydraulic diameter (DH), vulnerability index (VI) and potential specific stem conductivity (K_p); and wood water-use efficiency (iWUE), carbon isotope discrimination $\Delta^{13}C$ (‰) and C_i (ppm) of as physiological characteristics. We also included tree identity nested in study site as a random effect. RW, K_p, VI, C_i, $\Delta^{13}C$ and DBH were log-transformed prior to analysis to meet assumptions of normality.

Availability of data and materials
Data will be made available on request.

Declarations

Ethics approval and consent to participate
Not applicable.

Consent for publication
Not applicable.

Competing interests
The authors declare that they have no known competing financial interests or personal relationships that could have appeared to influence the work reported in this paper.

Author details
[1]Hémera Centro de Observación de la Tierra, Universidad Mayor, Camino La Pirámide 5750, Huechuraba, Santiago, Chile. [2]GEMA Center for Genomics, Ecology and Environment, Universidad Mayor, Camino La Pirámide 5750, Huechuraba, Santiago, Chile. [3]Data Observatory Foundation, ANID Technology Center, Eliodoro Yáñez 2990, 7510277 Providencia, Santiago, Chile. [4]Department of Forest Sciences, ESALQ-University of Sao Paulo, Pádua Dias Avenue 11, Piracicaba, Brazil. [5]Department of Plant Biology, Institute of Biology, University of Campinas, Monteiro Lobato, 255, Cidade Universitária, Campinas, Brazil. [6]Instituto de Geografía, Universidad Nacional Autónoma de México (UNAM), Circuito de la, Investigación Científica, 04510 Ciudad de Mexico, México. [7]Argentine Institute of Nivology, Glaciology and Environmental Sciences (IANIGLA CONICET), Dr. Ruiz Leal S/N-Parque General San Martín, M5500 Mendoza, Argentina. [8]Institute of Geography, Pontificia Universidad Católica de Valparaíso, Brasil Avenue 2241, 2362807 Valparaíso, Chile. [9]Instituto de Ciencias Agroalimentarias, Animales y Ambientales (ICA3), Universidad de O'Higgins, Ruta 90 Km 3, San Fernando 90, Chile.

References
Alvarez-Garreton C, Boisier JP, Garreaud R, Seibert J, Vis M (2021) Progressive water deficits during multiyear droughts in basins with long hydrological memory in Chile. Hydrol Earth Syst Sci 25:429–446. https://doi.org/10.5194/hess-25-429-2021

Andreu-Hayles L, Planells O, Gutierrez E, Muntan E, Helle G, Anchukaitis KJ, Schleser GH (2011) Long tree-ring chronologies reveal 20th century increases in water-use efficiency but no enhancement of tree growth at five Iberian pine forests. Glob Chang Biol 17:2095–2112. https://doi.org/10.1111/j.1365-2486.2010.02373.x

Arroyo MTK, Robles V, Tamburrino Í, Martínez-Harms J, Garreaud RD, Jara-Arancio P, Pliscoff P, Copier A, Arenas J, Keymer J, Castro K (2020) Extreme drought affects visitation and seed set in a plant species in the central Chilean Andes heavily dependent on hummingbird pollination. Plants 9:1553. https://doi.org/10.3390/plants9111553

Barichivich J, Sauchyn DJ, Lara A (2009) Climate signals in high elevation tree-rings from the semiarid Andes of north-central Chile: responses to regional and large-scale variability. Palaeogeogr Palaeoclimatol Palaeoecol 281:320–333. https://doi.org/10.1016/j.palaeo.2007.10.033

Bates D, Mächler M, Bolker B, Walker S (2015) Fitting linear mixed-effects models using lme4. J Stat Softw 67:1–48. https://doi.org/10.18637/jss.v067.i01

Beeckman H (2016) Wood anatomy and trait-based ecology. IAWA J 37:127–151. https://doi.org/10.1163/22941932-20160127

Bryukhanova M, Fonti P (2013) Xylem plasticity allows rapid hydraulic adjustment to annual climatic variability. Trees 27:485–496. https://doi.org/10.1007/s00468-012-0802-8

Carlquist S (1977) Ecological factors in wood evolution: a floristic approach. Am J Bot 64:886–896. https://doi.org/10.1002/j.1537-2197.1977.tb11932.x

Carrer M, von Arx G, Castagneri D, Petit G (2015) Distilling allometric and environmental information from time series of conduit size: the standardization issue and its relationship to tree hydraulic architecture. Tree Physiol 35:27–33. https://doi.org/10.1093/treephys/tpu108

Castagneri D, Carrer M, Regev L, Boaretto E (2020) Precipitation variability differently affects radial growth, xylem traits and ring porosity of three Mediterranean oak species at xeric and mesic sites. Sci Total Environ 699:134285. https://doi.org/10.1016/j.scitotenv.2019.134285

Cavieres L, Valencia G, Hernández C (2021) Calentamiento global y sus efectos en plantas de alta-montaña en Chile central: una revisión. Ecosistemas 30:2179. https://doi.org/10.7818/ECOS.2179

Cernusak LA, Ubierna N (2022) Carbon isotope effects in relation to CO_2 assimilation by tree canopies. In: Siegwolf RTW, Brooks JR, Roden J, Saurer M (eds) Stable isotopes in tree rings. Tree Physiology, vol 8. Springer, Cham. https://doi.org/10.1007/978-3-030-92698-4_9

Cherubini P, Battipaglia G, Innes JL (2021) Tree vitality and forest health: can tree-ring stable isotopes be used as indicators? Curr Rep 7:69–80. https://doi.org/10.1007/s40725-021-00137-8

Santini Jr. *et al. Ecological Processes*   (2024) 13:10

Page 11 of 12

Choat B, Cobb AR, Jansen S (2008) Structure and function of bordered pits: new discoveries and impacts on whole-plant hydraulic function. New Phytol 177:608–626. https://doi.org/10.1111/j.1469-8137.2007.02317.x

Choat B, Jansen S, Brodribb TJ et al (2012) Global convergence in the vulnerability of forests to drought. Nature 491:752–755. https://doi.org/10.1038/nature11688

Colangelo M, Camarero JJ, Gazol A et al (2021) Mediterranean old-growth forests exhibit resistance to climate warming. Sci Total Environ 801:149684. https://doi.org/10.1016/j.scitotenv.2021.149684

Cook BI, Smerdon JE, Cook ER et al (2022) Megadroughts in the common era and the anthropocene. Nat Rev Earth Environ 3:741–757. https://doi.org/10.1038/s43017-022-00329-1

Cuny HE, Rathgeber CBK, Frank D et al (2015) Woody biomass production lags stem-girth increase by over one month in coniferous forests. Nat Plants 1:15160. https://doi.org/10.1038/nplants.2015.160

De Kort H, Panis B, Helsen K, Douzet R, Janssens SB, Honnay O (2020) Pre-adaptation to climate change through topography-driven phenotypic plasticity. J Ecol 108:1465–1474. https://doi.org/10.1111/1365-2745.13365

Fonti P, von Arx G, Garcia-Gonzalez I et al (2010) Studying global change through investigation of the plastic responses of xylem anatomy in tree rings. New Phytol 185:42–53. https://doi.org/10.1111/j.1469-8137.2009.03030.x

García-Cervigón AI, Olano JM, von Arx G, Fajardo A (2018) Xylem adjusts to maintain efficiency across a steep precipitation gradient in two coexisting generalist species. Ann Bot 122:461–472. https://doi.org/10.1093/aob/mcy088

Garcia-Gonzalez I, Souto-Herrero M, Campelo F (2016) Ring-porosity and early-wood vessels: a review on extracting environmental information through time. IAWA J 37:295–314. https://doi.org/10.1163/22941932-20160135

Garreaud RD, Boisier JP, Rondanelli R, Montecinos A, Sepúlveda H, Veloso-Aguila D (2020) The central Chile mega drought (2010–2018): a climate dynamics perspective. Int J Climatol 40:421–439. https://doi.org/10.1002/joc.6219

Gärtner H, Nievergelt D (2010) The core-microtome: a new tool for surface preparation on cores and time series analysis of varying cell parameters. Dendrochronologia 28:85–92. https://doi.org/10.1016/j.dendro.2009.09.002

Gazol A, Camarero JJ, Sánchez-Salguero R et al (2022) Tree growth response to drought partially explains regional-scale growth and mortality patterns in Iberian forests. Ecol Appl 32:e2589. https://doi.org/10.1002/eap.2589

Gea-Izquierdo G, Fonti P, Cherubini P, Martin-Bentino D, Chaar H, Cañellas I (2012) Xylem hydraulic adjustment and growth response of *Quercus canariensis* Willd. to climatic variability. Tree Physiol 32:401–413. https://doi.org/10.1093/treephys/tps026

Gennaretti F, Carrer M, García-González I, Rossi S, von Arx G (2022) Quantitative wood anatomy to explore tree responses to global change. Front Plant Sci 13:e998895. https://doi.org/10.3389/fpls.2022.998895

Gleason SM, Westoby M, Jansen S et al (2016) Weak tradeoff between xylem safety and xylem-specific hydraulic efficiency across the world's woody plant species. New Phytol 209:123–136. https://doi.org/10.1111/nph.13646

González-Reyes Á, Jacques-Coper M, Bravo C, Rojas M, Garreaud R (2023) Evolution of heatwaves in Chile since 1980. Weather Clim Extrem 41:e100588. https://doi.org/10.1016/j.wace.2023.100588

Granda E, Rossatto DR, Camarero JJ, Voltas J, Valladares F (2014) Growth and carbon isotopes of Mediterranean trees reveal contrasting responses to increased carbon dioxide and drought. Oecologia 174:307–317. https://doi.org/10.1007/s00442-013-2742-4

Granda E, Gazol A, Camarero JJ (2018) Functional diversity differently shapes growth resilience to drought for co-existing pine species. J Veg Sci 29:265–275. https://doi.org/10.1111/jvs.12617

Grissino-Mayer HD (2001) Evaluating crossdating accuracy: a manual and tutorial for the computer program COFECHA. Tree-Ring Res 57:205–221

Hacke UG, Sperry JS (2001) Functional and ecological xylem anatomy. Perspect Plant Ecol Evol Syst 4:97–115. https://doi.org/10.1078/1433-8319-00017

Hacke UG, Sperry JS, Wheeler JK, Castro L (2006) Scaling of angiosperm xylem structure with safety and efficiency. Tree Physiol 26:689–701. https://doi.org/10.1093/treephys/26.6.689

Hentschel R, Rosner S, Kayler ZE, Hentschel R, Rosner S, Kayler ZE, Andreassen K, Børja I, Solberg TO, Priesack E, Gessler A (2014) Norway spruce

physiological and anatomical predisposition to dieback. For Ecol Manage 322:27–36. https://doi.org/10.1016/j.foreco.2014.03.007

Hersbach H, Bell B, Berrisford P et al (2020) The ERA5 global reanalysis. Q J R Meteorol Soc 146(730):1999–2049. https://doi.org/10.1002/qj.3803

Körner C, Hoch G (2023) Not every high-latitude or high-elevation forest edge is a treeline. J Biogeogr 50(4):838–845. https://doi.org/10.1111/jbi.14593

Lavergne A, Sandoval D, Hare VJ, Graven H, Prentice IC (2020) Impacts of soil water stress on the acclimated stomatal limitation of photosynthesis: insights from stable carbon isotope data. Glob Chang Biol 26:7158–7172. https://doi.org/10.1111/gcb.15364

Lavergne A, Hemming D, Prentice IC, Guerrieri R, Oliver RJ, Graven H (2022) Global decadal variability of plant carbon isotope discrimination and its link to gross primary production. Glob Chang Biol 28:524–541. https://doi.org/10.1111/gcb.15924

Lens F, Sperry JS, Christman MA, Choat B, Rabaey D, Jansen S (2011) Testing hypotheses that link wood anatomy to cavitation resistance and hydraulic conductivity in the genus *Acer*. New Phytol 190:709–723. https://doi.org/10.1111/j.1469-8137.2010.03518.x

Lévesque M, Siegwolf R, Saurer M, Eilmann B, Rigling A (2014) Increased water-use efficiency does not lead to enhanced tree growth under xeric and mesic conditions. New Phytol 203:94–109. https://doi.org/10.1111/nph.12772

Li C, Leal Filho W, Wang J, Yin J, Fedoruk M, Bao G, Bao Y, Yin S, Yu S, Hu R (2018) An assessment of the impacts of climate extremes on the vegetation in Mongolian Plateau: using a scenarios-based analysis to support regional adaptation and mitigation options. Ecol Indic 95:805–814. https://doi.org/10.1016/j.ecolind.2018.08.031

Linares JC, Camarero JJ (2012) From pattern to process: linking intrinsic water-use efficiency to drought-induced forest decline. Glob Chang Biol 18:1000–1015. https://doi.org/10.1111/j.1365-2486.2011.02566.x

López R, Cano FJ, Rodríguez-Calcerrada J, Sangüesa-Barreda G, Gazol A, Camarero JJ, Rozenberg P, Gil L (2021) Tree-ring density and carbon isotope composition are early-warning signals of drought-induced mortality in the drought tolerant Canary Island pine. Agric For Meteorol 310:e108634. https://doi.org/10.1016/j.agrformet.2021.108634

Lüdecke D, Patil I, Ben-Shachar MS, Wiernik BM, Waggoner P, Makowski D (2021) see: An R package for visualizing statistical models. J Open Source Softw 6:3393. https://doi.org/10.21105/joss.03393

Martínez-Ferri E, Balaguer L, Valladares F, Chico JM, Manrique E (2000) Energy dissipation in drought-avoiding and drought-tolerant tree species at midday during the Mediterranean summer. Tree Physiol 20:131–138. https://doi.org/10.1093/treephys/20.2.131

Martínez-Vilalta J, García-Valdés R, Jump A, Vilà-Cabrera A, Mencuccini M (2023) Accounting for trait variability and coordination in predictions of drought-induced range shifts in woody plants. New Phytol 240(1):23–40. https://doi.org/10.1111/nph.19138

Mathias JM, Hudiburg TW (2022) isocalcR: An R package to streamline and standardize stable isotope calculations in ecological research. Glob Chang Biol 28:7428–7436. https://doi.org/10.1111/gcb.16407

Matskovsky V, Venegas-González A, Garreaud R, Roig F, Gutierrez A, Muñoz AA, Le Quesne C, Klock K, Canales C (2021) Tree growth decline as a response to projected climate change in the 21st century in Mediterranean mountain forests of Chile. Glob Planet Change 198:e103406. https://doi.org/10.1016/j.gloplacha.2020.103406

McDowell NG, Sapes G, Pivovaroff A, Adams H, Allen CD, Anderegg W, Arend M, Breshears DD, Brodribb T, Choat C, Cochard H, De Cáceres M, De Kauwe M, Grossiord C, Hammond W, Hartmann H, Hoch G, Kahmen A, Klein T, Mackay DS, Mantova M, Martínez-Vilalta J, Medlyn B, Mencuccini M, Nardini A, Oliveira RS, Sala A, Tissue D, Torres-Ruiz JM, Trowbridge A, Trugman A, Wiley E, Xu C (2022) Mechanisms of woody-plant mortality under rising drought, CO_2 and vapour pressure deficit. Nat Rev Earth Environ 3:294–308. https://doi.org/10.1038/s43017-022-00272-1

Miranda A, Lara A, Altamirano A, Di Bella C, González ME, Camarero JJ (2020) Forest browning trends in response to drought in a highly threatened Mediterranean landscape of South America. Ecol Indic 115:106401. https://doi.org/10.1016/j.ecolind.2020.106401

Morales MS, Cook ER, Barichivich J et al (2020) Six hundred years of South American tree rings reveal an increase in severe hydroclimatic events since mid-20th century. Proc Natl Acad Sci USA 117:16816–16823. https://doi.org/10.1073/pnas.2002411117

Santini Jr. *et al. Ecological Processes*   (2024) 13:10

Page 12 of 12

Mrad A, Domec J, Huang C, Huang CW, Lens F, Katul G (2018) A network model links wood anatomy to xylem tissue hydraulic behaviour and vulnerability to cavitation. Plant Cell Environ 41:2718–2730. https://doi.org/10.1111/pce.13415

Nola P, Bracco F, Assini S, von Arx G, Castagneri D (2020) Xylem anatomy of *Robinia pseudoacacia* L. and *Quercus robur* L. is differently affected by climate in a temperate alluvial forest. Ann Sci 77:1–16. https://doi.org/10.1007/s13595-019-0906-z

Pellizzari E, Camarero JJ, Gazol A, Sangüesa-Barreda G, Carrer M (2016) Wood anatomy and carbon-isotope discrimination support long-term hydraulic deterioration as a major cause of drought-induced dieback. Glob Chang Biol 22:2125–2137. https://doi.org/10.1111/gcb.13227

Peñuelas J, Lloret F, Montoya R (2001) Severe drought effects on Mediterranean woody flora in Spain. For Sci 47:214–218. https://doi.org/10.1093/forestscience/47.2.214

Peñuelas J, Canadell JG, Ogaya R (2011) Increased water-use efficiency during the 20th century did not translate into enhanced tree growth. Glob Ecol Biogeogr 20:597–608. https://doi.org/10.1111/j.1466-8238.2010.00608.x

Pepin N, Bradley RS, Diaz HF, Caceres EB, Forsythe N, Fowler H, Greenwood G, Hashmi MZ, Liu XD, Ning L, Ohmura A, Palazzi E, Rangwala I, Schoner W, Seversky I, Shahgedanova M, Wand MB, Williamson SN, Yang DQ (2015) Elevation-dependent warming in mountain regions of the world. Nat Clim Change 5:424–430. https://doi.org/10.1038/nclimate2563

Piper FI, Cavieres LA, Reyes-Díaz M, Corcuera LJ (2006) Carbon sink limitation and frost tolerance control performance of the tree Kageneckia angustifolia D. Don (Rosaceae) at the treeline in central Chile. Plant Ecol 185:29–39

Pittermann J, Choat B, Jansen S, Stuart S, Lynn L, Dawson T (2010) The relationships between xylem safety and hydraulic efficiency in the Cupressaceae: the evolution of pit membrane form and function. Plant Physiol 153:1919–1931. https://doi.org/10.1104/pp.110.158824

Puchi PF, Camarero JJ, Battipaglia G, Carrer M (2021) Retrospective analysis of wood anatomical traits and tree-ring isotopes suggests site-specific mechanisms triggering *Araucaria araucana* drought-induced dieback. Glob Chang Biol 27:6394–6408. https://doi.org/10.1111/gcb.15881

Quintilhan MT, Santini L Jr, Rodriguez DRO, Guillemot J, Marangom G, Chambi-Legoas R, Bouvellon Y, Tomazello-Filho M (2021) Growth-ring boundaries of tropical tree species: aiding delimitation by long histological sections and wood density profiles. Dendrochronologia 69:e125878. https://doi.org/10.1016/j.dendro.2021.125878

R Core Team (2020) R: a language and environment for statistical computing. Foundation for Statistical Computing, Vienna, Austria

Rodríguez-Ramírez EC, Ferrero ME, Acevedo-Vega I, Crispin-DelaCruz D, Ticse-Otarola G, Requena-Rojas E (2022) Plastic adjustments in xylem vessel traits to drought events in three *Cedrela* species from Peruvian Tropical Andean forests. Sci Rep 12:e21112. https://doi.org/10.1038/s41598-022-25645-w

Santini L Jr, Rodriguez DRO, Quintilhan MT, Brazolin S, Tomazello-Filho M (2019) Evidence to wood biodeterioration of tropical species revealed by non-destructive techniques. Sci Total Environ 672:357–369. https://doi.org/10.1016/j.scitotenv.2019.03.429

Saurer M, Voelker S (2022) Intrinsic water-use efficiency derived from stable carbon isotopes of tree-rings. In: Siegwolf RTW, Brooks JR, Roden J, Saurer M (eds) Stable isotopes in tree rings. Tree Physiology, vol 8. Springer, Cham, pp 481–498. https://doi.org/10.1007/978-3-030-92698-4_17

Schmitz N, Jansen S, Verheyden A, Gitundu Kairo J, Beeckman H, Koedam N (2007) Comparative anatomy of intervessel pits in two mangrove species growing along a natural salinity gradient in Gazi Bay, Kenya. Ann Bot 100:271–281. https://doi.org/10.1093/aob/mcm103

Seager R, Osborn TJ, Kushnir Y, Simpson I, Nakamura J, Liu H (2019) Climate variability and change of Mediterranean-type climates. J Clim 32:2887–2915. https://doi.org/10.1175/JCLI-D-18-0472.1

Sperry JS, Nichols KL, Sullivan JEM, Eastlack SE (1994) Xylem embolism in ring-porous, diffuse-porous, and coniferous trees of northern Utah and interior Alaska. Ecology 75:1736–1752. https://doi.org/10.2307/1939633

Sperry JS, Hacke UG, Pittermann J (2006) Size and function in conifer tracheids and angiosperm vessels. Am J Bot 93:1490–1500. https://doi.org/10.3732/ajb.93.10.1490

Sterck FJ, Zweifel R, Sass-Klaassen U, Chowdhury Q (2008) Persisting soil drought reduces leaf specific conductivity in Scots pine (*Pinus sylvestris*)

and pubescent oak (*Quercus pubescens*). Tree Physiol 28:529–536. https://doi.org/10.1093/treephys/28.4.529

Stokes MA, Smiley TL (1968) An introduction to tree-ring dating. University of Chicago Press, Chicago

Tovar C, Carril AF, Gutiérrez AG, Ahrends A, Fita L, Zaninelli P, Flombaum P, Abarzúa AM, Alarcón D, Aschero V, Báez S, Barros A, Carilla J, Ferrero ME, Flantua S, Gonzáles P, Menéndez C, Pérez-Escobar O, Pauchard A, Ruscica R, Särkinen T, Sörensson A, Srur A, Villalba R, Hollingsworth PM (2022) Understanding climate change impacts on biome and plant distributions in the Andes: challenges and opportunities. J Biogeogr 49:1420–1442. https://doi.org/10.1111/jbi.14389

Venegas-González A, Roig FA, Gutiérrez AG, Tomazello Filho M (2018) Recent radial growth decline in response to increased drought conditions in the northernmost *Nothofagus* populations from South America. For Ecol Manage 409:94–104. https://doi.org/10.1016/j.foreco.2017.11.006

Venegas-González A, Mello FNA, Schnitzer SA, Cesar R, Tomazello-Filho M (2020) The negative effect of lianas on tree growth varies with tree species and season. Biotropica 52:836–844. https://doi.org/10.1111/btp.12796

Venegas-González A, Munoz AA, Carpintero-Gibson S, González-Reyes A, Schneider I, Gipolou-Zuñiga T, Aguilera-Betti I, Roig F (2023) Sclerophyllous forest tree growth under the influence of a historic megadrought in the Mediterranean Ecoregion of Chile. Ecosystems 26:344–361. https://doi.org/10.1007/s10021-022-00760-x

von Arx G, Crivellaro A, Prendin AL, Kufar K, Carrer M (2016) Quantitative wood anatomy—practical guidelines. Front Plant Sci 7:e781. https://doi.org/10.3389/fpls.2016.00781

Weigt RB, Bräunlich S, Zimmermann L, Saurer M, Grams T, Dietrich H, Siegwolf R, Nikolova P (2015) Comparison of $\delta^{18}O$ and $\delta^{13}C$ values between tree-ring whole wood and cellulose in five species growing under two different site conditions. Rapid Commun Mass Spectrom 29:2233–2244. https://doi.org/10.1002/rcm.7388

Wheeler JK, Sperry JS, Hacke UG, Hoang N (2005) Inter-vessel pitting and cavitation in woody Rosaceae and other vesselled plants: a basis for a safety versus efficiency trade-off in xylem transport. Plant Cell Environ 28:800–812. https://doi.org/10.1111/j.1365-3040.2005.01330.x

Wu G, Liu X, Chen T, Xu G, Wang W, Zeng X, Zhang X (2015) Elevation-dependent variations of tree growth and intrinsic water-use efficiency in Schrenk spruce (*Picea schrenkiana*) in the western Tianshan Mountains, China. Front Plant Sci 6:e309. https://doi.org/10.3389/fpls.2015.00309

Xu X, Jiang H, Guan M, Wang L, Huang Y, Jiang Y, Wang A (2020) Vegetation responses to extreme climatic indices in coastal China from 1986 to 2015. Sci Total Environ 744:e140784. https://doi.org/10.1016/j.scitotenv.2020.140784

Zhang W-W, Song J, Wang M, Liu Y, Li N, Zhang Y, Holbrook NM, Hau G (2017) Divergences in hydraulic architecture form an important basis for niche differentiation between diploid and polyploid *Betula* species in NE China. Tree Physiol 37:604–616. https://doi.org/10.1093/treephys/tpx004

Zwieniecki MA, Secchi F (2015) Threats to xylem hydraulic function of trees under 'new climate normal' conditions. Plant Cell Environ 38:1713–1724. https://doi.org/10.1111/pce.12412

Publisher's Note